LDPC Codes for Flat Rayleigh Fading Channels with Channel Side Information

Yibo Jiang, Alexei Ashikhmin, Naresh Sharma

Abstract— **In this paper, we design capacity approaching low-density parity-check (LDPC) codes in the low signal-to-noise ratio (SNR) regime for flat Rayleigh fading channels with channel side information at transmitter and receiver. We use the structure advocated by Caire et al, which uses a single codebook with dynamic power allocation. The extrinsic information transfer (EXIT) function method is used to design the LDPC codes which approach the channel capacities. We also study the EXIT function properties of various demappers, and consider the error exponents in the high SNR regime.**

Index Terms— **low-density parity-check (LDPC) codes, mutual information, iterative decoding, fading, channel side information.**

Y. Jiang is with Coordinated Science Laboratory, University of Illinois at Urbana-Champaign, Urbana, IL 61801, USA. Email: yjiang@uiuc.edu

A. Ashikhmin is with Bell Laboratories, Lucent Technologies, 600 Mountain Avenue, Murray Hill, NJ 07974, USA. Email: aea@research.bell-labs.com

N. Sharma is with Open Innovations Lab, Lucent Technologies, 67 Whippany Rd., Whippany, NJ 07981, USA. Email: nereshs@lucent.com

I. Introduction

In the field of wireless communications, numerous papers have been devoted to designing capacity approaching codes for fading channels with channel state information (CSI) at the receiver, e.g., [1], [2]. For uncorrelated flat Rayleigh fading channel, at rate 0.5, the irregular LDPC code designed in [1] has a threshold 0.07 dB away from the channel capacity. On the other hand, for flat fading channels with perfect CSI at transmitter and receiver, there are only a limited number of papers in the literature about capacity approaching codes design. In [3], optimal power allocation and an expression for the channel capacity of a fading channel with channel side information were derived. To prove the coding theorem, the authors of [3] used a scheme in which the system encoder multiplexes a sequence of codebooks with different rates and average powers determined by the fading level. The system decoder demultiplexes the channel out-

puts to the corresponding individual decoders. Some of the later work on practical coding schemes design is based on this variable-rate variable-power idea. For example, in [4], trellis coded adaptive M-ary quadrature amplitude modulation (M-QAM) schemes were proposed, which combine coset codes with adaptive M-QAM. For adaptive modulation technique, see [5], [6] and the reference therein. For some simple trellis codes, effective coding gains of around 4 dB were reported in [4]. However, they are still about 6 dB away from capacity. In [7], adaptive turbo-coded modulation (TuCM) was proposed, where both the turbo encoders and the modulation schemes were adapted to channel fading. It was reported in [7] that the TuCM schemes come within 3 dB of channel capacity. In the TuCM system, discrete rate adaption is employed, and in each rate region, different encoding and decoding schemes are used. Thus the complexity of design and implementation is relatively high.

In [8], the authors proposed a simple scheme to achieve the capacity of fading channel with CSI at transmitter and receiver. It consists of a single rate and power Gaussian codebook and a power allocator. At the receiver side, there is only one decoder. Thus, instead of multiple variable-rate and variable-power codebooks [3], one Gaussian codebook is enough to achieve the capacity (refer to [9] for an excellent review). Intuitively, we believe that if the Gaussian random code is replaced by a carefully designed LDPC code (plus some fixed modulation scheme), the performance should still be very close to the capacity limit. In this paper, we follow this line of thought and focus on designing good LDPC codes to approach the channel capacity in the low SNR regime. Compared to previous designs which are mainly based on the idea of [3], one of the advantage of our scheme is the simple structure and simple implementation.

To design LDPC codes, we use the EXIT function methods in [10], [11], which essentially matches the EXIT curves of variable node decoder (VND) and check node decoder (CND) to optimize the degree distribution. We design an LDPC code with rate $r \approx 0.15$ and quadrature phase-shift keying (QPSK) modulation, which is 0.98 dB away from the Shannon limit of the fading channel with CSI at transmitter and receiver and with QPSK modulation. We also design an LDPC code with rate $r \approx 0.2137$ and 16-QAM modulation, which is 0.167 dB away from the Shannon limit of the fading channel with CSI at transmitter and receiver and with 16-QAM modulation.

According to the EXIT function method, in the case of M-QAM modulation with $M > 4$, for designing a good LDPC code one should take into account the shape of the EXIT func-

tion of a particular demapper. In this paper we study and compare the EXIT functions of various demappers and make several interesting observations, e.g., on the area property of demapper EXIT functions.

It is well known that in the high SNR regime, channel side information at the transmitter provides negligible gain in channel capacity. We explore its impact on the error exponent. Based on the study of LDPC codes design in this regime, we make the conjecture that in the high SNR regime, the error exponent of fading channel with CSI at transmitter and receiver is very close to the error exponent of fading channel with CSI at receiver only, when the code rate is close to the channel capacity.

Thus, we conjecture that in the high SNR regime knowledge of CSI at the transmitter not only give little gain in terms of capacity, but also does not allow one to significantly reduce the probability of error.

Several abbreviations are frequently used in this paper. CSI TR stands for the channel with CSI at transmitter and receiver, CSI R stands for the channel with CSI at receiver.

The paper is organized as follows. In section II, we describe the channel models used in this paper and introduce some important information theoretic results. In section III, we give a short description of the EXIT functions design method. In section IV, we design LDPC codes for transmission with QPSK modulation. In section V, we study the EXIT functions of various demappers , and design LDPC codes for transmission with 16-QAM modulation. Section VI considers code design in the high SNR regime and error exponents. Section VII concludes this paper.

II. Channel Models and Information Theoretic Aspects

We consider a discrete-time i.i.d. flat Rayleigh fading channel with channel state information perfectly known at both transmitter and receiver. Let S be the average transmit power, N_0 be noise density, B be the bandwidth, and h_i be the fading coefficient at time instant i. Define $\gamma_i = Sh_i^2/(N_0B)$. Since the transmitter knows CSI, it can adjust transmit power $S(\gamma)$ subject to an average power constraint

$$\int_\gamma S(\gamma)p(\gamma)d\gamma \leq S \tag{1}$$

In [3], it is determined that the optimal power control formula has the following water-filling type

$$\frac{S(\gamma)}{S} = \begin{cases} \frac{1}{\gamma_0} - \frac{1}{\gamma} & \text{if } \gamma \geq \gamma_0 \\ 0 & \text{if } \gamma < \gamma_0 \end{cases} \tag{2}$$

where γ_0 is a solution to

$$\int_{\gamma_0}^{\infty} (\frac{1}{\gamma_0} - \frac{1}{\gamma})p(\gamma)d\gamma = 1. \tag{3}$$

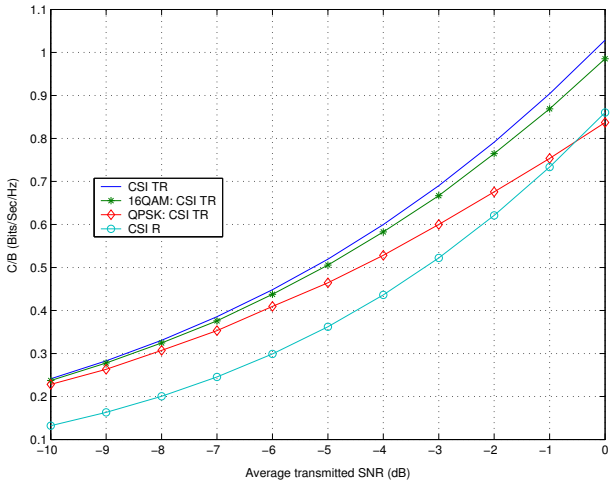


Fig. 1. Capacities for the CSI TR and CSI R fading channels, and mutual information for QPSK and 16-QAM modulations in the CSI TR fading channel, all in the low SNR regime.

Thus the power constraint is satisfied with equality, and the average transmitted SNR is $\frac{S}{N_0 B}$. The capacity formula corresponding to the optimal power allocation is also obtained in [3]

$$C = \int_{\gamma_0}^{\infty} B \log(\frac{\gamma}{\gamma_0}) p(\gamma) d\gamma. \qquad (4)$$

In the case when CSI is known at the receiver only, the channel capacity is [3]

$$C = \int B \log(1+\gamma) p(\gamma) d\gamma \qquad (5)$$

It is well known that in the high SNR regime, especially when SNR is bigger than 15 dB, the difference between the capacity of a CSI TR fading channel and the capacity of a CSI R fading channel is negligible [3]. Thus, the codes designed for approaching the capacity of a CSI R fading channel can be used to approach the capacity of a CSI TR fading channel.

On the other hand, in the low SNR regime, the capacity gap between two channels can be significant. For instance, for SNR in the interval between -10 dB and 0 dB the gap varies from 1.5 dB to 3 dB, as shown in Fig. 1.

This motivates us to consider the problem of designing capacity approaching codes for a CSI TR fading channel in the low SNR regime. In Fig. 1 we also plot the mutual information functions $I(X;Y)$ for QPSK and 16-QAM modulations in the CSI TR fading channel (denoted by "QPSK: CSI TR" and "16QAM: CSI TR" respectively), where X is a QPSK symbol or a 16-QAM symbol, Y is the output of the fading channel, and the power of transmitted symbols is scaled according to Eq. (2).

According to Fig. 1, at very low SNR, for instance when it is less than -7 dB, we can use QPSK modulation and still be relatively close to the CSI TR channel capacity. At higher SNR it is better to use 16-QAM modulation. Below we illustrate the code design for these two types of modulations.

III. The EXIT functions design method

This method of EXIT functions or charts was suggested by S. ten Brink [12] for designing turbo codes. In [10], [13] the method was

extended for design of LDPC codes and a rigorous analysis of the method was conducted for the case of the binary erasure channel (BEC). We give a short description of the method for the sake of completeness.

The idea of this method is the following. We define the VND and CND EXIT functions, $I_E^{VND}(I_A, I_C)$ and $I_E^{CND}(I_A)$, for variable and check nodes of an LDPC code respectively. These functions show how the mutual information changes during the variable and check nodes processing at each iteration of the belief propagation decoding. The function I_E^{VND} depends on the degree distribution λ_i of variable nodes (from the edges perspective) of the LDPC code. The function I_E^{CND} depends on degree distribution ρ_i of check nodes (from the edges perspective). Let $I_A^{CND}(I_E)$ be the inverse function of $I_E^{CND}(I_A)$. In [10], the following results are proven for the case of BECs

- for successful belief propagation decoding the VND EXIT function should stay above the inverse CND EXIT function, i.e. $I_E^{VND}(I_A = x, I_C) \geq I_A^{CND}(I_E = x), x \in [0, 1]$;
- the smaller gap between the VND EXIT function and the inverse CND EXIT function the closer the code rate to the channel capacity.

Although these results are not exact for channels different from BEC, they still can be used as a guideline for designing LDPC codes for a memoryless channel. For instance, these results were used in [11] for construction of capacity approaching LDPC codes in the case of multiple-input multiple-output ergodic fading channels. In the rest of this paper we will refer to both functions $I_E^{CND}(I_A)$ and $I_A^{CND}(I_E)$ as CND EXIT function. The meaning will be clear from the context.

Let us first outline the computational procedure for the case of binary-input additive white Gaussian noise (BIAWGN) channel. Let $Y = b + N$ be a BIAWGN channel, where b is an equiprobable binary symbol, N is the additive noise with zero mean and variance σ_n^2. The log-likelihood ratio (LLR) for that channel is

$$L_{ch} = \ln \frac{\Pr(b = 1|Y)}{\Pr(b = -1|Y)} = 2Y/\sigma_n^2,$$

thus the variance of L_{ch} is $\sigma_{ch}^2 = 4/\sigma_n^2$ and conditional mean value is $b\sigma_{ch}^2/2$. In [12], [11] the expression for the mutual information $I(b; Y) = J(\sigma_{ch})$ was derived. Assuming that messages entering a variable node of degree i are Gaussian distributed (one message is coming from the channel which has capacity I_c, and other $i-1$ messages are coming from check nodes), we can estimate the EXIT function

$I_{E,VND}(I_A, I_C, i)$ of the node as follows [11]

$$\begin{aligned} &I_{E,VND}(I_A, I_C, i) \\ =&J\left(\sqrt{(i-1)[J^{-1}(I_A)]^2 + J^{-1}(I_C)^2}\right) \end{aligned} \quad (6)$$

The EXIT function of an average variable node is

$$I_E^{VND}(I_A, I_C) = \sum_{i=1} \lambda_i \cdot I_{E,VND}(I_A, I_C, i) \quad (7)$$

Again assuming that messages entering a check node of degree i are Gaussian distributed (all messages are coming from variable nodes), we have the following expression for its EXIT function [14]

$$\begin{aligned} &I_{E,CND}(I_A, i) \\ =&\frac{1}{\ln 2} \sum_{j=1}^{\infty} \frac{1}{(2j)(2j-1)} [\mathrm{E}(T^{2j})]^{i-1}, \end{aligned} \quad (8)$$

where

$$\mathrm{E}[T^{2j}] = \int_{-1}^{1} \frac{2t^{2j}}{(1-t^2)\sqrt{4\pi m}} e^{\frac{-(\ln \frac{1+t}{1-t} - m)^2}{4m}} dt$$

and

$$m = \frac{1}{2}\left(J^{-1}(I_A)\right)^2.$$

In [15] an even more precise version of the EXIT function method was suggested. In practice, however, it is more convenient to use the following simple approximation, which is based on the duality theorem from [10] and was used in [11], for $I_{E,CND}(I_A, i)$:

$$I_{E,CND}(I_A, i) \approx 1 - J\left(\sqrt{i-1} \cdot J^{-1}(1 - I_A)\right). \quad (9)$$

As it is demonstrated in [14] the difference between (9) and (8) is negligible. From (8) we obtain

$$I_E^{CND}(I_A) = \sum_i \rho_i I_{E,CND}(I_A, i).$$

We will consider construction of LDPC codes whose check nodes have a constant degree d_c. We will also assume that the maximum variable node degree can not exceed some value $d_{v,max}$. Let A_i be the area between $I_{E,VND}(I_A, I_C, i)$ and $I_{A,CND}(I_E, d_c)$, where $I_{A,CND}(I_E, d_c)$ is the inverse function of $I_{E,CND}(I_A, d_c)$. The problem of matching the VND and CND EXIT functions is equivalent to solving the following linear programming problem

$$\min \sum_{i=1}^{d_{v,max}} \lambda_i A_i, \quad (10)$$

$$\sum_{i=1}^{d_{v,max}} \lambda_i I_{E,VND}(x, I_C, i) \;\geq\; I_{A,CND}(x, d_c),$$

where $x \in [0, 1]$. Thus the optimal degree distribution $\lambda_1, \ldots, \lambda_{d_{v,max}}$ can be numerically obtained by linear programming algorithms.

In the following two sections we present an application of this method for construction of good LDPC codes for transmission with QPSK and 16-QAM modulations in the CSI TR fading channel.

IV. LDPC CODES DESIGN WITH QPSK MODULATION

According to Fig.1, in the case of very low SNR the mutual information of QPSK mod-

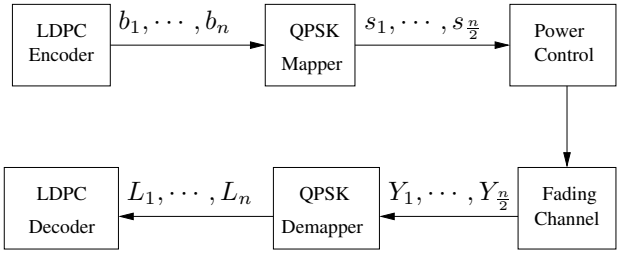


Fig. 2. The coding and decoding scheme when QPSK modulation is used.

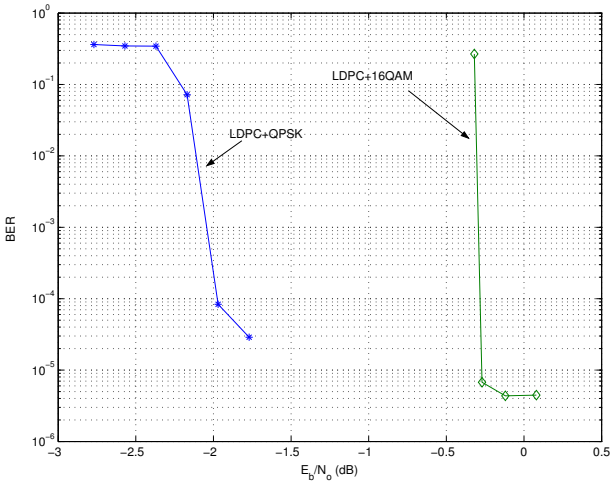


Fig. 3. The BER performance of an LDPC code with QPSK modulation ("LDPC+QPSK") , and another LDPC code with 16-QAM modulation ("LDPC+16QAM").

ulation in a CSI TR fading channel, "QPSK: CSI TR", is very close to the Shannon capacity of the CSI TR fading channel. Taking into account this observation, we propose the following simple practical coding and decoding scheme shown in Fig. 2. The LDPC encoder produces a codeword $(b_1, b_2, \ldots, b_n)$, for each pair of codeword bits $b_{2i-1}, b_{2i}, i = 1, \cdots, n/2$, the QPSK mapper chooses a QPSK signal s_i, and the power controller allocates the power for s_i according to (2).

We assume that the QPSK mapper uses the Gray mapping. The QPSK demapper computes log-likelihood ratios for all codeword bits

$$L_j = \ln\left(\frac{\Pr(b_j = 0|Y_{\lceil \frac{j}{2} \rceil})}{\Pr(b_j = 1|Y_{\lceil \frac{j}{2} \rceil})}\right), j = 1, \cdots, n.$$

It is easy to see that this transmission is equivalent to the transmission of two independent BPSK signals. This means that knowledge of one bit assigned to a QPSK signal does not carry any information about the other bit assigned to the signal. For this reason any feedback from the LDPC decoder to the QPSK demapper does not help demapping and therefore the QPSK demapper is not included into decoding iterations in Fig.2.

In an AWGN channel, the output LLRs of a BPSK demodulator are conditionally Gaussian distributed. In a CSI TR fading channel, like in Fig. 2, the LLRs L_i at the output of the QPSK demapper is not exactly Gaussian. However, we can still treat it as a Gaussian distribution with variance $J^{-1}(I_C)^2$. Then we can use the EXIT function design method in the same way as for the BIAWGN channel.

Finding a good feasible solution of the linear programming problem (10), we construct an LDPC code with rate $R = 15834/105834 \approx$

0.15 and length $n = 105834$. All check nodes of the code have degree 4 and the degree distribution of variable nodes is

$$\lambda_2 = 0.3720,\ \lambda_3 = 0.1480,\ \lambda_4 = 0.1110,$$
$$\lambda_5 = 0.0830,\ \lambda_{20} = 0.2860. \tag{11}$$

The results of simulation of this code with the belief propagation decoding with 200 iterations are shown in Fig. 3 (indicated by "LDPC+QPSK"). The code achieves BER of 10^{-4} at $E_b/N_o = -1.98$ dB. From the plots in Fig. 1, one can see that the Shannon limit for the channel "CSI TR" is $E_b/N_o = -3.46$ dB, and the Shannon limit for the channel "QPSK:CSI TR" is $E_b/N_o = -2.96$ dB. Thus, our code is 1.48 dB away from the Shannon limit of the fading channel with CSI at transmitter and receiver, and 0.98 dB away from the Shannon limit of the fading channel with CSI at transmitter and receiver and with QPSK modulation.

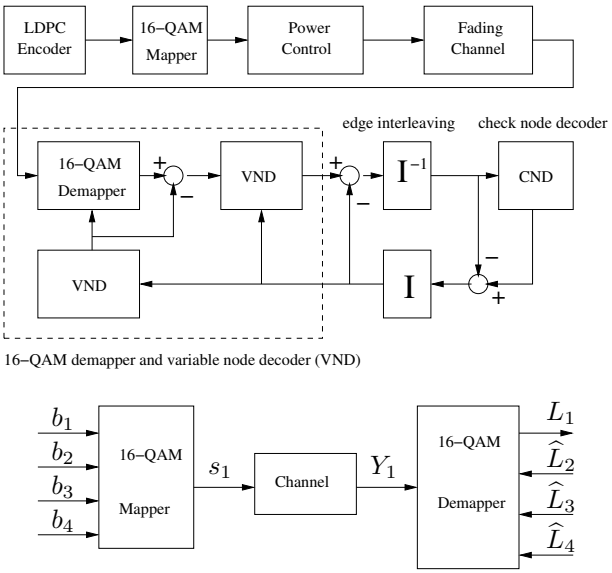


Fig. 4. Top part: the coding and decoding scheme when 16-QAM modulation is used. Bottom part: the model for simulating the EXIT function of a 16-QAM demapper.

V. LDPC CODES DESIGN WITH 16-QAM MODULATION

A. Comparison of the EXIT Functions of Demappers

In this section, we consider the design of LDPC codes when 16-QAM modulation is used. The 16-QAM mapper puts in correspondence to each 4-tuple $(b_{4i-3}, b_{4i-2}, b_{4i-1}, b_{4i})_{i=1}^{n/4}$ of codeword bits a signal from the 16-QAM constellation. Let us assume that we have prior estimates $\widehat{b}_{4i-3}, \widehat{b}_{4i-2}, \widehat{b}_{4i-1}, \widehat{b}_{4i}$ for corresponding codeword bits. It is not difficult to see that in this case

$$I(b_{4i-j}; Y_i) \ \leq \ I(b_{4i-j}; Y_i | \widehat{b}_{4i-j_1}, \widehat{b}_{4i-j_2}, \widehat{b}_{4i-j_3}),$$
$$j_1, j_2, j_3 \ \neq \ j.$$

For this reason the 16-QAM Demapper is included in the decoding iteration process as shown in the top part of Fig.4. After each decoding iteration between variable and check nodes of the LDPC code, the variable nodes pass new estimates of the code bits in the form of LLRs $\widehat{L}_i$ to the 16-QAM demapper.

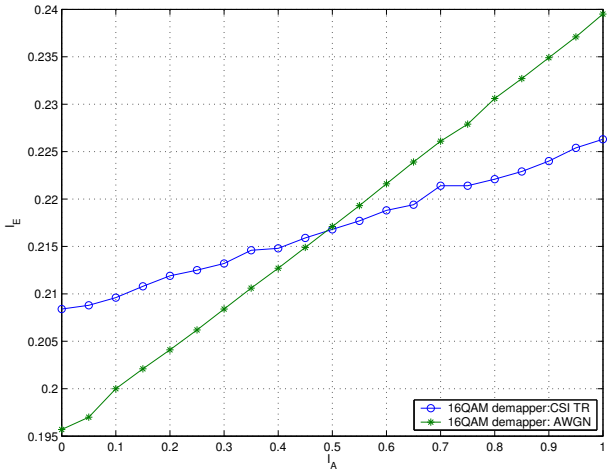


Fig. 5. The EXIT functions comparison of a 16-QAM demapper in a CSI TR fading channel with average transmitted SNR -1 dB, and an AWGN channel with SNR -0.7813 dB.

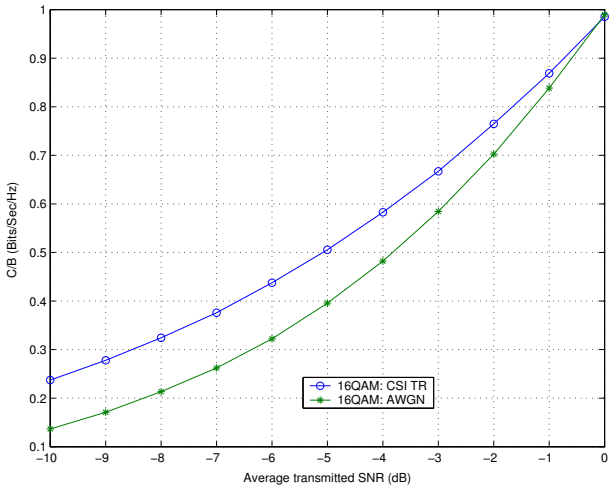


Fig. 6. Capacity curves for fading channel with CSI at transmitter and receiver and 16-QAM input (denoted by "16QAM: CSI TR"), and AWGN channel with 16-QAM input (denoted by "16QAM: AWGN").

Each $\widehat{L}_i$ is computed as the sum of LLRs coming to the i-th variable node (of degree $d_{v,i}$) from check nodes. The density of $\widehat{L}_i$ is usually approximated by a Gaussian density. Numerical experiments show that this approximation is quite accurate. Thus we assume that conditioned on $b_i = \pm 1$, $\widehat{L}_i$ is a Gaussian random variable with variance $d_{v,i}J^{-1}(I_A)^2$ and conditional mean value $\pm d_{v,i}J^{-1}(I_A)^2/2$. (An explanation for choosing the mean of $\widehat{L}_i$ to be half of its variance can be found in [14],[16].)

In the bottom part of Fig. 4 we plot a block diagram for the simulation of mutual information

$$I_{E,1}(I_A) = I(b_1; L_1) = I(b_1; Y_1 | \widehat{L}_2, \widehat{L}_3, \widehat{L}_4).$$

The average mutual information of a 16-QAM demapper is computed as

$$I_E(I_A) = \frac{1}{4}(I_{E,1}(I_A) + I_{E,2}(I_A) + I_{E,3}(I_A) + I_{E,4}(I_A)).$$

(For all 4-tuple $(b_{4i-3}, b_{4i-2}, b_{4i-1}, b_{4i})$ of the codeword bits the computation of $I_E(I_A)$ is the same.) On Fig. 5 the result of the simulation of the EXIT function $I_E(I_A)$ of the 16-QAM demapper in the CSI TR fading channel is presented when the average transmitted SNR is equal to -1 dB.

On Fig. 6 we plot the capacity of "16QAM: CSI TR" transmission and the capacity of a 16-QAM modulation in an AWGN channel (denoted by "16QAM: AWGN"). From these plots one can see that the capacity of "16QAM:

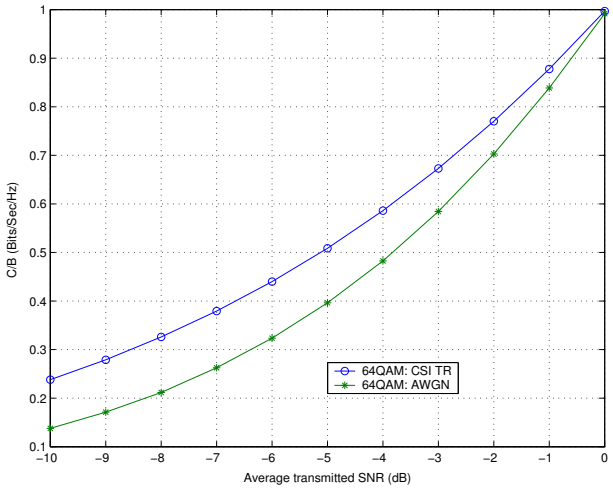


Fig. 7. Capacity curves for fading channel with CSI at transmitter and receiver and 64-QAM input (denoted by "64QAM: CSI TR"), and AWGN channel with 64-QAM input (denoted by "64QAM: AWGN").

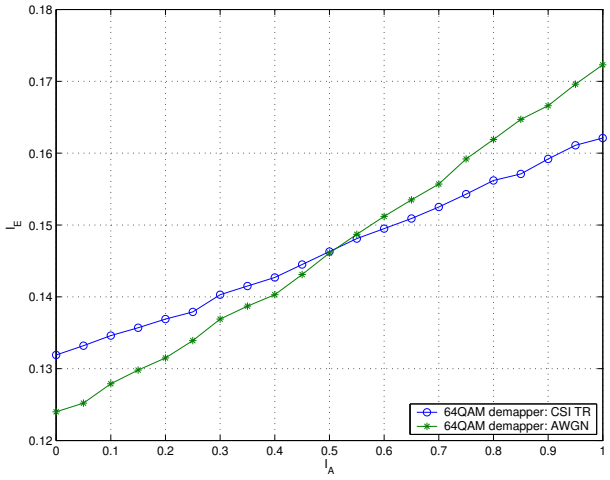


Fig. 8. The EXIT functions comparison of a 64-QAM demapper in a CSI TR fading channel with average transmitted SNR -1 dB, and an AWGN channel with SNR -0.75 dB.

AWGN" at SNR -0.7813 dB is approximately equal to 0.8689 Bits/Sec/Hz, i.e. the capacity of "16QAM: CSI TR" at -1 dB. It is instructive to construct the EXIT function $I_E(I_A)$ of the 16-QAM demapper for this AWGN channel, which is shown in Fig. 5. One can see the EXIT function of the 16-QAM demapper in the case of an AWGN channel is steeper than in the case of a CSI TR fading channel. Thus we conclude that we have to choose *different* degree distributions for construction of capacity approaching LDPC codes in these two cases.

It is also interesting to note that the areas under the two functions in Fig. 5 are approximately the same, which is probably due to the fact that both channels have the same capacity (see Conjecture 1 below).

We are also interested in exploring whether the EXIT functions of demappers become steeper as the size of modulation increases. To this end, we consider the 64-QAM modulation. Assuming the average transmitted SNR is -1 dB, we simulate the EXIT function of a 64-QAM demapper in a CSI TR fading channel, and plot it in Fig. 8 (denoted by "64QAM demapper: CSI TR"). One can see that the function is steeper compared to the 16-QAM case. Similarly, from Fig. 7, we know that for a CSI TR fading channel with 64-QAM modulation, the capacity at -1 dB is 0.8766 Bits/Sec/Hz, and for an AWGN channel with 64-QAM input to have that capacity value, the SNR should be -0.75 dB. We also simulate

the EXIT function for the latter case and plot it in Fig. 8 (denoted by "64QAM demapper:AWGN"). Again, one can observe that the demapper EXIT function in the AWGN case is steeper, and the areas under two functions are approximately equal.

In general let us assume that we transmit information with the help of a signal constellation of size M and the capacity of our communication scheme is equal to C. Let A denote the area under the EXIT function of the corresponding demapper. Then we make the following conjecture.

Conjecture 1: $C \approx A \cdot \log_2(M)$.

For example, in the case of a 16-QAM demapper, $\mathrm{M} = 16$, $\mathrm{A} = 0.2175$, thus $\mathrm{A} \cdot \log_2(\mathrm{M}) = 0.87$, which is very close to the capacity value 0.8689. In the case of a 64-QAM demapper, $\mathrm{M} = 64$, $\mathrm{A} = 0.147$, thus $\mathrm{A} \cdot \log_2(\mathrm{M}) = 0.882$, which is also quite close to the capacity value 0.8766.

Conjecture 1 is also related to the following result from [10]. Let us assume that we transmit codewords $\underline{x}$ of an $[n, k]$ error correcting code and receive vectors $\underline{y}$. Let us also assume that some prior estimates of the k *information* symbols of $\underline{x}$ are available to the *a posteriori* probability (APP) decoder of the code. Let us finally compute the average mutual information $I_E(I_A)$ between the information symbols of $\underline{x}$ and corresponding outputs of the APP decoder for a given value of the average mutual information I_A between the information symbols of $\underline{x}$ and the prior estimates of these symbols. In Example 10 (p. 2662, [10]) it is proven that in the case of BEC the area under $I_E(I_A)$ equals to

$$A = 1 - H(\underline{x}|\underline{y})/k = \frac{I(\underline{x};\underline{y})/n}{R}, \qquad (12)$$

where $R = k/n$ is the code rate. One can draw an analogy between transmission with the help of a modulation of constellation size M and the described scenario. To draw the analogy we replace $I(\underline{x}, \underline{y})$ by the capacity of a given modulation constellation, and $nR = k$ by $\log_2(M)$. Bits that are mapped into a modulation symbol play the role of the information symbols of the vector $\underline{x}$, and the received signal Y plays the role of $\underline{y}$. We think that Conjecture 1 can be useful for numerical estimation of the channel capacities in the case of complex communication channels and modulation constellations.

B. Code Design and Simulation Results

We follow the method which is described in [11, Sec.III]. In order to obtain a combined demapper and VND function in closed form, we approximate the EXIT function of the 16-QAM demapper shown in Fig. 5 by a third-order polynomial

$$I_E = 0.2082 + 0.0173 \cdot I_A - 0.0001 \cdot I_A^2 + 0.0008 \cdot I_A^3. \qquad (13)$$

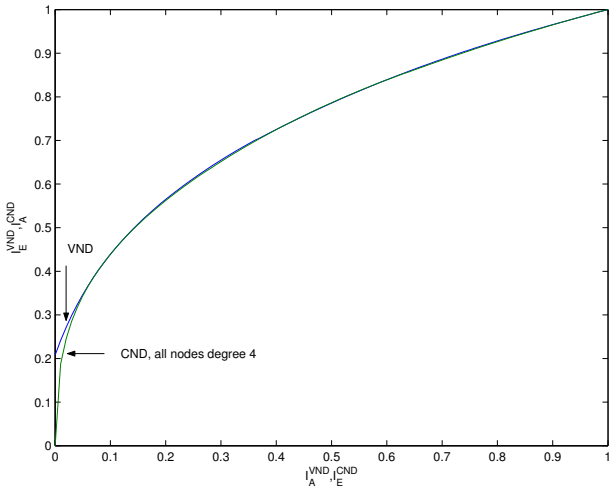


Fig. 9. Combined 16-QAM demapper/VND function (VND) and CND function corresponding to the designed degree distribution.

Then using Eq. (6) and (13), we can easily combine the EXIT functions of the 16-QAM demapper and VND into a new function, essentially combining three components inside the box in Fig. 4 into a single component.

Now, the design problem is essentially the same as in the QPSK case. We want to match the combined EXIT function of the 16-QAM demapper and VND with the EXIT function of the CND. The optimal degree distribution vector can be obtained numerically by linear programming algorithms. As a result, we design an LDPC code with rate $R = 20385/95385 \approx 0.2137$, codeword length $n = 95385$. All check nodes of the code have degree 4 and the degree distribution of the variable nodes is

$$\lambda_2 = 0.396,\ \lambda_3 = 0.228,\ \lambda_6 = 0.0891,\ \lambda_7 = 0.1589,\ \lambda_{20} = 0.128. \tag{14}$$

The combined 16-QAM demapper/VND function and CND function corresponding to the designed degree distribution are shown in Fig. 9. We simulate the BER performance of belief propagation decoding of this code which is shown in Fig. 3 (indicated by "LDPC+16QAM"). The number of iterations is 200. The code achieves BER of 10^{-4} at $E_b/N_o = -0.283$ dB. From the plots in Fig. 1, one can see that the Shannon limit for the channel "CSI TR" is $E_b/N_o = -0.73$ dB, and the Shannon limit for the channel "16QAM:CSI TR" is $E_b/N_o = -0.45$ dB. Thus, our code is 0.447 dB away from the Shannon limit of the CSI TR fading channel and 0.167 dB away from the Shannon limit of transmission through the CSI TR fading channel with 16-QAM modulation.

VI. Code design in the high SNR regime

It is well known that in the high SNR regime, channel side information at the transmitter provides negligible gain in channel capacity. One can ask a question whether it provides significant reduction of the probability of error. In connection with that we simulate the EXIT functions of 64-QAM demappers in the high

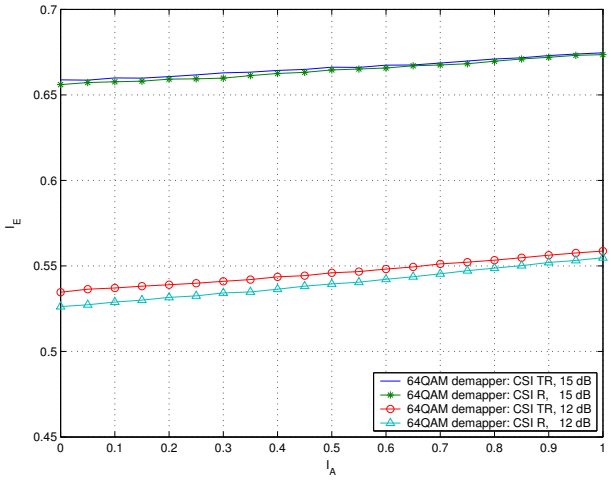


Fig. 10. The EXIT functions of 64-QAM demappers in the high SNR regime: 12 dB and 15 dB. For each SNR, EXIT functions are simulated for two channel models: CSI TR, and CSI R.

SNR regime, for two channel models: CSI TR, and CSI R. From Fig. 10, we would like to note that the EXIT functions for two channel models with the same SNR are very close to each other, which is especially true for 15 dB SNR. From this it follows that the degree distributions optimized by the EXIT function method for the CSI TR and CSI R channels will also be very close to each other. Hence the performance of corresponding LDPC codes will also be almost the same. Thus we make the following conjecture.

Conjecture 2: In the high SNR regime, the capacity approaching LDPC codes for the CSI TR and CSI R channels have almost the same probability of error.

One can also observe that in the high SNR regime the optimal power allocation (2) is becoming very flat, in other words it becomes very close to the constant power allocation. Taking this into account, we make the following conjecture.

Conjecture 3: In the high SNR regime, the error exponents of CSI TR and CSI R fading channels are very close to each other when the code rate is close to the channel capacity.

VII. CONCLUSION

In this paper, we have used the single codebook with dynamic power allocation structure from [8], and designed two capacity approaching LDPC codes, with QPSK and 16-QAM modulation respectively. We have also studied the EXIT functions property of various demappers, and made some interesting observations on the areas under the EXIT functions. We have also discussed the code design in the high SNR regime, and made the conjecture that in the high SNR regime, the error exponents of CSI TR and CSI R channels are very close to each other when the code rate is close to the channel capacity. One of the future work is to study the code design for non-ergodic fading, especially with delay constraint. Paper [17] studied the variable-rate coding for a non-ergodic multiple-access Gaussian block fading channel, but is more from an information theoretic perspec-

tive. One may consider more practical code designs.

ACKNOWLEDGMENT

The authors would like to thank Eran Sharon for his Matlab file which was used in our simulation programs, and Uri Erez, Xinzhou Wu for helpful discussions.

REFERENCES

[1] J. Hou, P. Siegel, and L. Milstein, "Performance analysis and code optimization of low density parity-check codes on Rayleigh fading channels," *IEEE J. Select. Areas Commun.*, vol. 19, no. 5, pp. 924–934, May 2001.

[2] E. Hall and S. Wilson, "Design and analysis of turbo codes on Rayleigh fading channels," *IEEE J. Select. Areas Commun.*, vol. 16, no. 2, pp. 160–174, Feb. 1998.

[3] A. J. Goldsmith and P. P. Varaiya, "Capacity of fading channels with channel side information," *IEEE Trans. Inform. Theory*, vol. 43, no. 6, pp. 1986–1992, Nov. 1997.

[4] A. Goldsmith and S. Chua, "Adaptive coded modulation for fading channels," *IEEE Trans. Commun.*, vol. 46, no. 5, pp. 595–602, May 1998.

[5] ——, "Variable-rate variable-power MQAM for fading channels," *IEEE Trans. Commun.*, vol. 45, no. 10, pp. 1218–1230, Oct. 1997.

[6] S. Chung and A. Goldsmith, "Degrees of freedom in adaptive modulation: a unified view," *IEEE Trans. Commun.*, vol. 49, no. 9, pp. 1561–1571, Sept. 2001.

[7] S. Vishwanath and A. Goldsmith, "Adaptive turbo-coded modulation for flat-fading channels," *IEEE Trans. Commun.*, vol. 51, no. 6, pp. 964–972, June 2003.

[8] G. Caire and S. Shamai, "On the capacity of some channels with channel state information," *IEEE Trans. Inform. Theory*, vol. 45, no. 6, pp. 2007–2019, Sept. 1999.

[9] E. Biglieri, J. Proakis, and S. Shamai, "Fading channels: information-theoretic and communications aspects," *IEEE Trans. Inform. Theory*, vol. 44, no. 6, pp. 2619–2692, Oct. 1998.

[10] A. Ashikhmin, G. Kramer, and S. ten Brink, "Extrinsic information transfer functions: Model and erasure channel properties," *IEEE Trans. Inform. Theory*, vol. 50, no. 11, pp. 2657–2673, Nov. 2004.

[11] S. ten Brink, G. Kramer, and A. Ashikhmin, "Design of low-density parity-check codes for modulation and detection," *IEEE Trans. Commun.*, vol. 52, no. 4, pp. 670–678, Apr. 2004.

[12] S. ten Brink, "Convergence behavior of iteratively decoded parallel concatenated codes," *IEEE Trans. Commun.*, vol. 49, no. 10, pp. 1727–1737, Oct. 2001.

[13] A. Ashikhmin, G. Kramer, and S. ten Brink, "Extrinsic information transfer functions: A model and two properties," in *Proc. Conf. Information Sciences and Systems*, Princeton, NJ, Mar. 2002, pp. 742–747.

[14] E. Sharon, A. Ashikhmin, and S. Litsyn, "EXIT functions for continuous channels: Part I. Constituent codes," *IEEE Trans. Commun.*, submitted for publication, 2004.

[15] ——, "EXIT functions for continuous channels: Part II. LDPC codes," *IEEE Trans. Commun.*, submitted for publication, 2004.

[16] T. J. Richardson, A. Shokrollahi, and R. Urbanke, "Design of capacity approaching irregular low-density parity-check codes," *IEEE Trans. Inform. Theory*, vol. 47, no. 2, pp. 619–637, Feb. 2001.

[17] G. Caire, D. Tuninetti, and S. Verdu, "Variable-rate coding for slowly-fading Gaussian multiple-access channels," *IEEE Trans. Inform. Theory*, submitted for publication, May, 2004.